

See discussions, stats, and author profiles for this publication at: <https://www.researchgate.net/publication/320029262>

# A bis-amide ruthenium polypyridyl complex as a robust and efficient photosensitizer for H<sub>2</sub> production

Article in ChemSusChem · September 2017

DOI: 10.1002/cssc.201701543

CITATIONS

7

READS

119

4 authors, including:



Garry S. Hanan

Université de Montréal

242 PUBLICATIONS 5,794 CITATIONS

[SEE PROFILE](#)



Amlan Kumar Pal

Indian Institute of Technology Jammu

57 PUBLICATIONS 955 CITATIONS

[SEE PROFILE](#)



Olivier Schott

Université de Montréal

13 PUBLICATIONS 137 CITATIONS

[SEE PROFILE](#)

Some of the authors of this publication are also working on these related projects:



Project

Covalently modified polyoxometalate with d6 metal photosensitizer [View project](#)



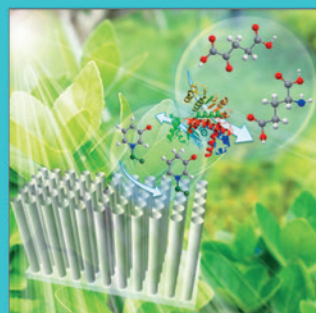
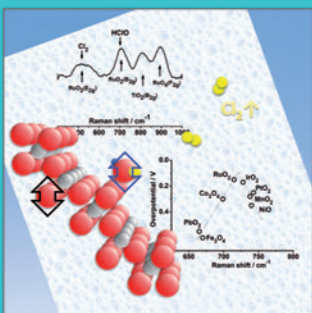
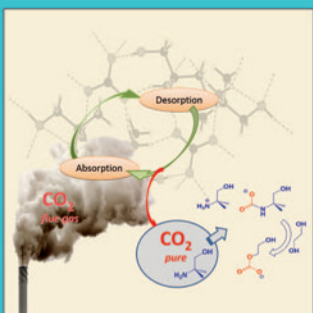
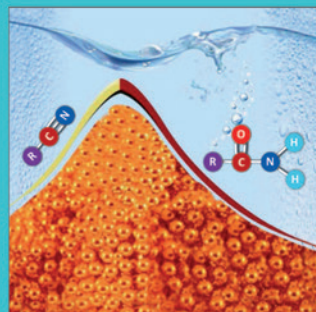
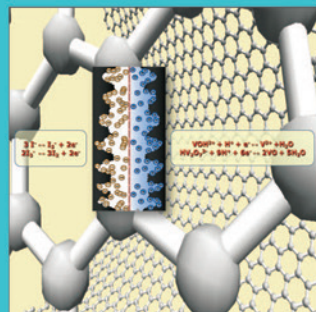
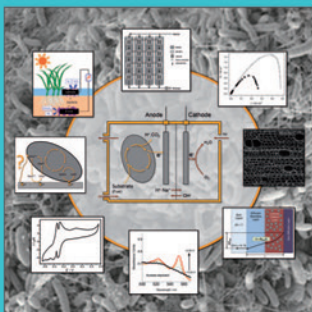
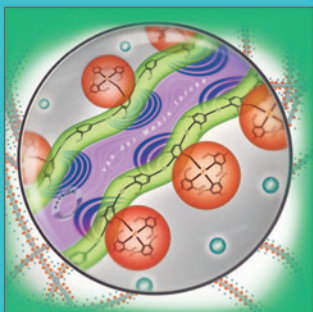
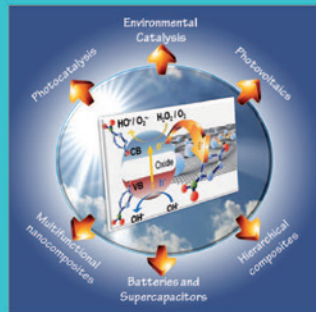
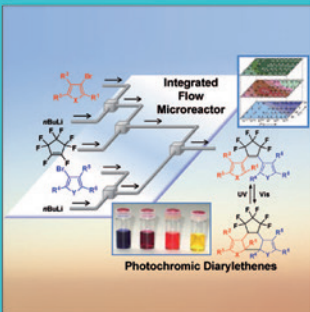
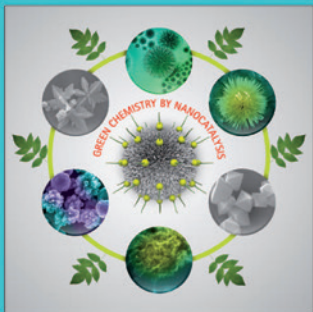
Project

supramolecular 3D architectures on surfaces [View project](#)

CHEMISTRY & SUSTAINABILITY

# CHEMSUSCHEM

ENERGY & MATERIALS



## Reprint

© Wiley-VCH Verlag GmbH & Co. KGaA, Weinheim

A Journal of



WILEY-VCH

[www.chemsuschem.org](http://www.chemsuschem.org)



# A Bisamide Ruthenium Polypyridyl Complex as a Robust and Efficient Photosensitizer for Hydrogen Production

Olivier Schott,<sup>[a]</sup> Amlan K. Pal,<sup>[a, b]</sup> Daniel Chartrand,<sup>[c]</sup> and Garry S. Hanan<sup>\*[a]</sup>

A photosensitizer based on a ruthenium complex of a bisamide-polypyridyl ligand gives rise to a large improvement in photocatalytic stability, rate of activity, and efficiency in photocatalytic H<sub>2</sub> production compared to [Ru(bpy)<sub>3</sub>]<sup>2+</sup> (bpy = 2,2'-bipyridine). The bisamide ruthenium polypyridyl complex combined with a cobaloxime-based photocatalyst was found to be highly efficient under blue-light (turnover number (TON) = 7800) and green-light irradiation (TON = 7200) whereas [Ru(bpy)<sub>3</sub>]<sup>2+</sup> was significantly less effective with a TON of 2600 and 1100, respectively. The greatest improvement was under red-light-emitting diodes, with bisamide ruthenium polypyridyl complex and cobaloxime exhibiting a TON of 4200 compared to [Ru(bpy)<sub>3</sub>]<sup>2+</sup> and cobaloxime at a TON of only 71.

The future well being of our society relies on innovative research to produce clean sources of energy. With global warming on the rise, new alternatives to fossil fuels are needed, and of the several options available, the inexhaustible power of the sun is one of the most convenient clean energy sources.<sup>[1]</sup> Molecular artificial photosynthesis presents a promising avenue for the conversion and storage of solar energy in chemical bonds as found in hydrogen gas.<sup>[2,3]</sup> Molecular photocatalytic systems for the hydrogen evolution reaction (HER), half of the water splitting process, are mainly composed of a photosensitizer (PS), a catalyst, and a sacrificial electron donor. In the last decade of photocatalytic research, Ir<sup>III</sup>,<sup>[4]</sup> Re<sup>I</sup>,<sup>[5]</sup> and Pt<sup>II</sup><sup>[6]</sup> were tested to improve the overall performance of the HER. In the case of PS made of d<sup>6</sup> metal complexes, many researchers uti-

lize the archetypical [Ru(bpy)<sub>3</sub>]<sup>2+</sup> (bpy = 2,2'-bipyridine) complex due to its lower cost and higher abundance of Ru compared to other transition-metal complexes.<sup>[7]</sup> To benefit from the availability of Ru-based PSs, however, some of its properties should be modified; for example, its absorption maximum at 450 nm should be shifted to longer wavelengths to take advantage of the tailing of the solar spectrum through the visible and near-IR regions.<sup>[7a, 8]</sup>

Among earth-abundant HER catalysts, new advances with Co catalysts<sup>[9]</sup> are particularly attractive compared to their Pt,<sup>[10]</sup> Pd,<sup>[11]</sup> and Rh<sup>[12]</sup> analogs. Cobaloximes are among the most studied molecular catalysts for H<sub>2</sub> production in electrocatalysis and photocatalysis.<sup>[4c, 6a, 7d, 9b-d, 13]</sup> For an efficient photocatalytic system, the PS and the catalyst must be in close proximity for efficient electron transfer; many assemblies exist that are covalently linked or connected by pendant pyridine (py) on the PS, which coordinates the catalysts.<sup>[4b, c, l, 8a, 14]</sup> Indeed, the better the electron transfer, the lesser is the probability of PS decomposition induced by ligand dissociation,<sup>[15]</sup> for example, the multi-metallic center-based supramolecular assembly Ru-Co<sub>6</sub> has better efficiency than the dissociated [Ru(bpy)<sub>3</sub>]<sup>2+</sup>-[Co(dmgH)<sub>2</sub>]<sup>+</sup> (dmgH = dimethylglyoxime) system.<sup>[8a, 14d]</sup> Charge-separated states and electronic transfer rates were also investigated through hydrogen-bonding or hydrophobic-interaction studies.<sup>[16]</sup> In this work, complex 1 (Figure 1) was investigated as a PS in combination with [Co(dmgH)<sub>2</sub>(DMAP)Cl] (3) (DMAP = 4-dimethylaminopyridine) as the photocatalyst to yield the pre-HER photocatalyst 4 (Figure 1). The photocatalytic H<sub>2</sub> production results were compared with that of archetypical [Ru(bpy)<sub>3</sub>]<sup>2+</sup> (2) as the PS and complex 3 as the photocatalyst. After the initial Co<sup>III</sup>-to-Co<sup>II</sup> reduction, the liberated chloride ion is available to bind in the pocket of PS 1, thus enhancing its properties as described by Beer et al. (vide infra).<sup>[17]</sup>

In the pioneering work of Beer et al., a family of optoelectronically active bisamide-based ruthenium complexes were developed for anion recognition.<sup>[17]</sup> Acyclic, macrocyclic, and calix[4]arene-substituted amide derivatives were tested to recognize halides.<sup>[17, 18]</sup> Herein, the ligand *N,N'*-diphenyl-[2,2'-bipyridine]-4,4'-dicarboxamide (L) in the heteroleptic Ru<sup>II</sup> complex 1 [bis(2,2'-bipyridine)(L)ruthenium(II) hexafluorophosphate] acts as a halide-ion receptor and can accommodate a chloride ion by non-classical hydrogen bonding with a stability constant of 40 L mol<sup>-1</sup>.<sup>[17]</sup> Furthermore, molar absorptivity of the <sup>1</sup>MLCT (metal-to-ligand charge transfer) band and emission intensity of complex 1 are enhanced as a result of chloride-ion recognition.<sup>[17]</sup> On this note, we decided to exploit the anion recognition<sup>[19]</sup> of complex 1 and the subsequent enhancement of photophysical properties for artificial photosynthesis. Complex 1 was investigated as a PS in combination with 3 as photocata-

[a] O. Schott, Dr. A. K. Pal, Prof. Dr. G. S. Hanan

Département de Chimie

Université de Montréal

2900 Edouard-Montpetit, Montréal, Québec H3T 1J4 (Canada)

Fax: (+1) 514-343-7586

E-mail: garry.hanan@umontreal.ca

[b] Dr. A. K. Pal

Organic Semiconductor Centre

EaStCHEM School of Chemistry

University of St Andrews

St Andrews, Fife KY16 9ST (United Kingdom)

[c] Dr. D. Chartrand

LAMP—Laboratoire d'Analyse pour les Molécules et Matériaux Photoactifs—Laboratory for the Analysis of Molecules' and Materials' Photoactivity

Université de Montréal

5155 Chemin de la Rampe, Montréal, Québec H3T 2B1 (Canada)

Supporting Information and the ORCID identification number(s) for the author(s) of this article can be found under <https://doi.org/10.1002/cssc.201701543>.

This publication is part of a Special Issue on the topic of Artificial Photosynthesis for Sustainable Fuels. To view the complete issue, visit: <http://dx.doi.org/10.1002/cssc.v10.22>.

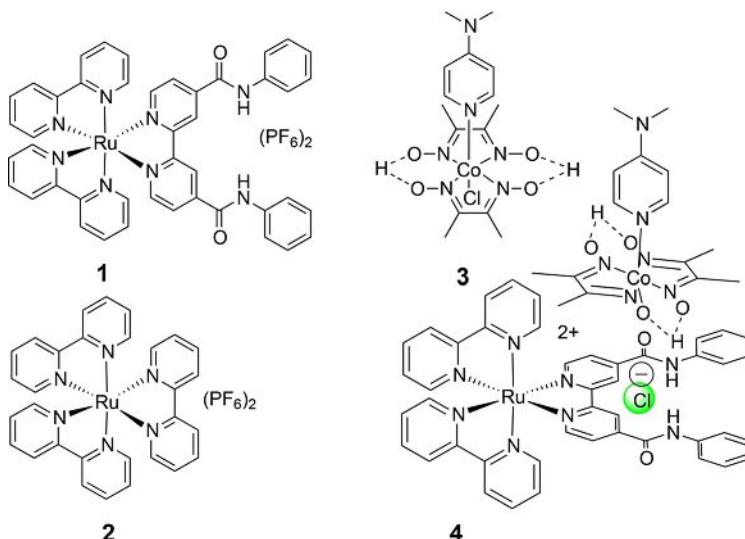


**Figure 1.** Molecular structures of Ru<sup>II</sup>-based PSs **1** and **2** and cobaloxime **3** used in this study; **4** describes the chloride anion transfer from **3** to **1** after reduction of the Co<sup>III</sup> complex.

lyst. The initial reduction of the Co<sup>III</sup> species leads to loss of the chloride anion, which enhances the photophysical properties of the PS.

Complex **1** (Figure 1) was prepared from [Ru(bpy)<sub>2</sub>Cl<sub>2</sub>] and ligand **L** as described by Beer et al.<sup>[17]</sup> It was characterized by <sup>1</sup>H and <sup>13</sup>C NMR spectroscopy (Figures S1a and S2 in the Supporting Information), high-resolution mass spectrometry, and elemental analysis. **3** was synthesized following a literature procedure.<sup>[13d]</sup> The formation of pre-HER catalyst **4** is supported by <sup>1</sup>H NMR studies of **1** and **3** (see the Supporting Information, Figure S1b), which revealed chemical shifts similar to those found previously.<sup>[17]</sup> Single crystals of **1** suitable for X-ray analysis were obtained by slow vapor diffusion of diethylether into a concentrated acetonitrile solution of complex **1**, prepared directly as its chloride salt (see Figures 2 and S3 in the Supporting Information for complete labelling). Selected crystallographic parameters are tabulated in Table S1 in the Supporting Information. A comparison of bond angles and distances obtained crystallographically and by density functional theory (DFT) calculation of complex **1** is tabulated in Table S2 in the Supporting Information. The coordinatively saturated Ru<sup>II</sup> center in complex **1** has a distorted octahedral geometry. The Ru–N distances for the coordinated bpy ligands are approximately the same for compound **1** (varies from 2.063(4) to 2.081(3) Å). These values are in line with the distances observed in Ru–bpy complexes in general (1.96–2.16 Å, average = 2.06(5) Å<sup>[20]</sup>). The chloride anion is encapsulated in the amide pocket of **L** in complex **1** through non-classical hydrogen bonding, as shown by Beer et al.<sup>[17]</sup>

The optoelectronic data for **1** and **2** are gathered in Table 1. In electrochemical experiments (Figure S4 and Table S3 in the Supporting Information) at positive potential, an anodic shift of 120 mV is observed for the first oxidation potential (Ru<sup>III</sup>/Ru<sup>II</sup>) of **1** ( $E_{1/2}^{\text{Ox}}=1.38$  V) compared to that of complex **2** ( $E_{1/2}^{\text{Ox}}=1.26$  V), in agreement with the lower energy calculated

for the highest occupied molecular orbital (HOMO) of complex **1** ( $E_{\text{HOMO}}=-6.24$  eV) compared to that of complex **2** ( $E_{\text{HOMO}}=-6.11$  eV) (Figure 3 and Tables S3 and S4). The first reduction potential of **1** ( $E_{1/2}^{\text{Red}}=-1.06$  V) is 270 mV less negative than that of **2** ( $E_{1/2}^{\text{Red}}=-1.33$  V), which is in line with the fact that the electron-withdrawing amide groups stabilize the lowest unoccupied molecular orbital (LUMO) of complex **1** compared to the same of reference complex **2** (calculated  $E_{\text{LUMO}}=-2.92$  and  $-2.54$  eV, respectively, for complexes **1** and **2**).

In the UV/Vis absorption spectra in Figure 4 several intense transitions in the high-energy region (<300 nm) are observed, which can be assigned to ligand-centered (LC) π–π\* transitions, as predicted by time-dependent (TD)-DFT calculations (Tables S5 and S6). The transitions between 300–450 nm are mostly related to singlet <sup>1</sup>MLCT transitions (either from Ru(dπ) to bpy(π\*) or Ru(dπ) to L(π\*)). The contribution of LC transitions is minor. The lowest energy transition at 476 nm is exclusively attributable to the

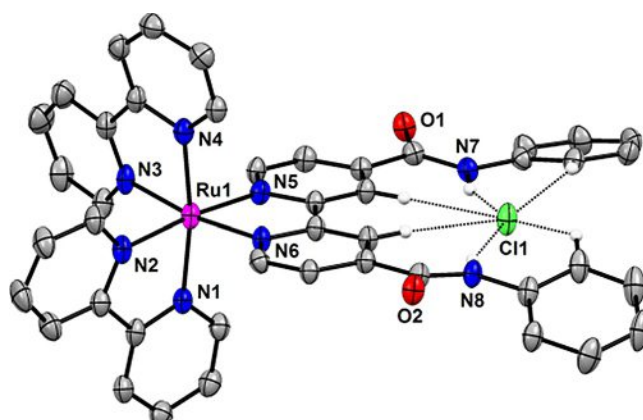


**Figure 2.** Oak Ridge thermal-ellipsoid plot (ORTEP) view of complex **1**. Ellipsoids correspond to a 50% probability level. Hydrogen atoms and one of the two chloride counter anions were omitted for clarity.

**Table 1.** Optoelectronic data of **1** and **2** in deaerated MeCN.<sup>[a]</sup>

Parameter	Compound <b>1</b>	Compound <b>2</b>
$E^{\text{ox}}$ [V] ( $\Delta E_p$ [mV])	1.38 (91) <sup>[b]</sup>	1.26 <sup>[21]</sup>
$E^{\text{red}}$ [V] ( $\Delta E_p$ [mV])	-1.06 (61) <sup>[b]</sup>	-1.33 <sup>[21]</sup>
$\Delta E_{\text{redox}}$ [V]	2.44	2.59
$\epsilon^{[c]}$ [ $10^3 \text{ L mol}^{-1} \text{ cm}^{-1}$ ]	15.7	14.6 <sup>[22]</sup>
$\lambda_{\text{abs}}^{[d]}$ [nm]	476	450
$\lambda_{\text{em}}^{[d]}$ [nm]	657	608 <sup>[22]</sup>
$\Phi_{\text{PL}}$ [%]	13	9.5 <sup>[23]</sup>
$\tau_{\text{PL}}$ [ns]	1200	870 <sup>[22]</sup>

[a] At room temperature. [b] Potentials are vs. standard calomel electrode, 0.1 M in [nBu<sub>4</sub>N]PF<sub>6</sub>, recorded at a sweep rate of 100 mVs<sup>-1</sup>. The difference between cathodic ( $E_{\text{pc}}$ ) and anodic ( $E_{\text{pa}}$ ) peak potentials ( $\Delta E_p$ ) is given in parentheses. [c] Molar absorptivity. [d]  $\lambda_{\text{abs}}$  = absorption wavelength;  $\lambda_{\text{em}}$  = emission wavelength.

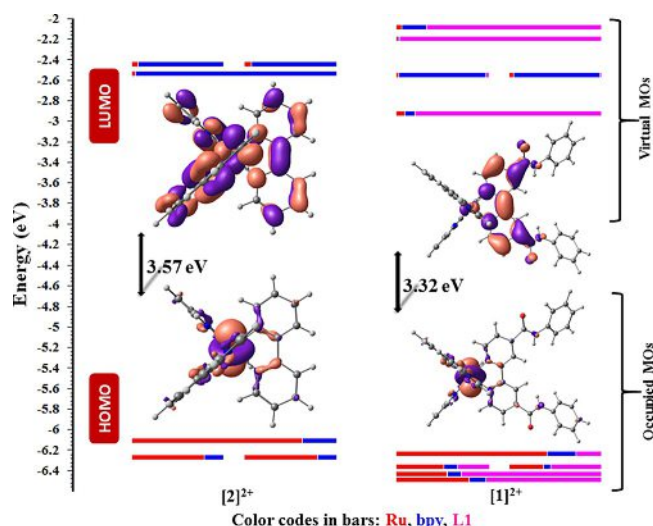


**Figure 3.** Calculated frontier molecular-orbital energies of  $[1]^{2+}$  and  $[2]^{2+}$ , obtained from TD-DFT (see Figure S5 for details).

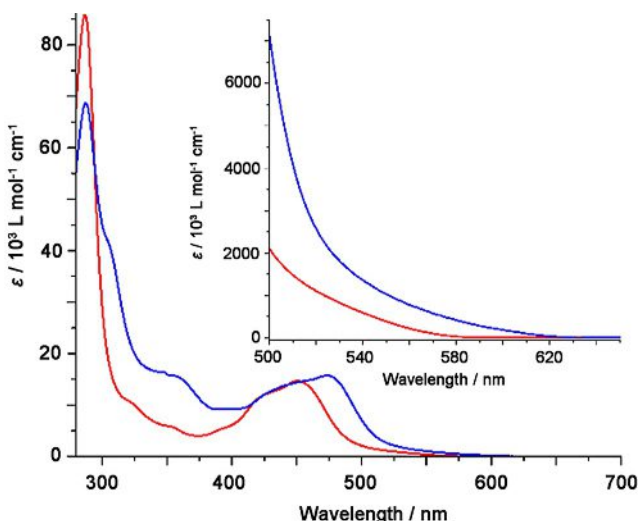


**Figure 4.** UV/Vis absorption spectra of **1** (blue) and **2** (red) in MeCN at 298 K. Inset: magnified spectra in the region from 500 to 650 nm.

$^1\text{MLCT}$  transition from  $\text{Ru}(\text{d}\pi)$  to  $\text{L}(\pi^*)$  as predicted by TD-DFT. In comparison to complex **2**, the lowest energy transition, which is  $\text{HOMO} \rightarrow \text{LUMO}$  in nature, is red-shifted by 26 nm as a result of stabilization of both the HOMO and LUMO in presence of electron-withdrawing amide functionality compared to those in **2**, thus reducing the overall HOMO-LUMO gap compared to the latter in **2** (Figure S5). The emission maximum wavelength of complex **1** ( $\lambda_{\text{em}} = 657 \text{ nm}$ ) in degassed MeCN solution at room temperature (RT) is red-shifted by 49 nm compared to that of complex **2** ( $\lambda_{\text{em}} = 608 \text{ nm}$ ) (Table 1 and Figure S7, the Supporting Information). The triplet spin density distribution (Figure S8, the Supporting Information) obtained from unrestricted DFT calculations of complex **1** suggests that the excited state is predominantly distributed on ligand **L** and the  $\text{Ru}^{II}$  ion as opposed to bpy; thus, the nature of emission can be attributed to the  $^3\text{MLCT}$  transition from  $\text{Ru}^{II}$  to **L**.

The photoluminescence quantum yield ( $\Phi_{\text{PL}}$ ) and the excited-state lifetime ( $\tau_{\text{PL}}$ ) values of complex **1** are increased to 13.3% and 1200 ns, respectively, in deaerated acetonitrile compared to those of the reference complex **2** ( $\Phi_{\text{PL}} = 9.5\%$  and  $\tau_{\text{PL}} = 870 \text{ ns}$ , Table 1). Considering its enriched optoelectronic properties, **1** appears to be a promising candidate to act as a PS for the HER.

Complex **1** was tested against complex **2** in parallel experiments for the photocatalytic HER (see the Supporting Information for experimental details). Recent studies revealed the influence of bpy on the catalyst activity of cobaloximes,<sup>[24]</sup> for example, the donating effect of DMAP on cobaloxime induces a fivefold higher HER rate than bpy in the complex  $[\text{Co}(\text{dmgh})_2(\text{py})\text{Cl}]$  in *N,N'*-dimethylformamide (DMF).<sup>[13d]</sup> However, the DMAP derivative demonstrates no photocatalytic activity in acidic aqueous media due to the strong electron-withdrawing character of the protonated dimethylamino moiety.<sup>[9d, 25]</sup> In our studies, the photoirradiation conditions used for DMF-TEOA (TEOA = triethanolamine) induce a basic medium ( $\text{pH}_{\text{apparent}} = 8.9$ ); thus, the DMAP substituent would exhibit a nucleophilic character. TEOA is used as a sacrificial electron donor (SED). As we recently reported for a Ru-Co<sub>6</sub> system, the photocatalytic activity and decomposition pathways of the reagents and catalysts depend on the wavelengths of irradiation.<sup>[8a]</sup>

In our studies, light-emitting diodes (LEDs) with  $\lambda_{\text{em}} = 452$ , 523, and 630 nm were used for  $\text{H}_2$  production (quantum yield calculations are shown in Figures S9–S11 in the Supporting Information). An overlap of the emissions of LEDs and the absorption spectra of PSs **1** and **2** were observed in all cases. Immediately after turning on the blue light, **1** photosensitizes the catalytic activity of catalyst **3** with a peak turnover frequency (TOF) of  $36000 \text{ mmol}_{\text{H}_2} \text{ mol}_{\text{PS}}^{-1} \text{ min}^{-1}$  ( $\Phi_{\text{H}_2} = 18.4\%$ ), which decreases to exhibit a turnover number (TON) of 7800 after 20 h (Figure 5). The reference system (**2** with **3**) provides a TOF of  $14000 \text{ mmol}_{\text{H}_2} \text{ mol}_{\text{PS}}^{-1} \text{ min}^{-1}$  ( $\Phi_{\text{H}_2} = 7.5\%$ ) and reaches a TON of 2600 after 20 h, one third of that of **1** with **3**.

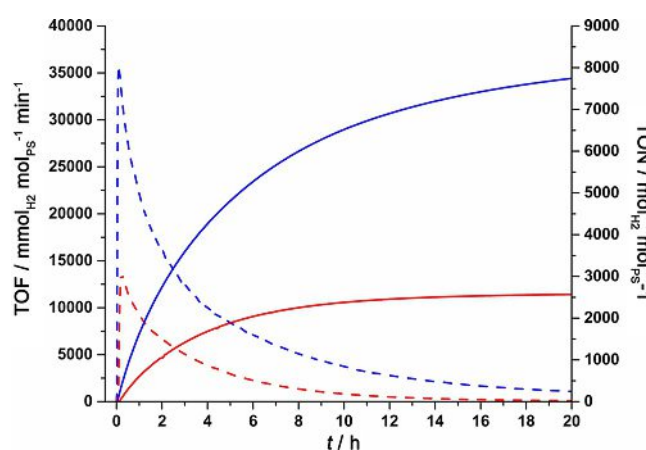


**Figure 5.**  $\text{H}_2$  evolution of  $(1-3) + 4$  equiv. dmgh₂ (blue) and reference system  $(2-3) + 4$  equiv. dmgh₂ (red). 1 M TEOA as SED and 0.1 M HBF<sub>4</sub> as proton source were used for both systems in DMF. Solid line: TON, dashed line: TOF. Irradiation at 452 nm (blue light).

Under green-light irradiation ( $\lambda_{\text{em}}=523 \text{ nm}$ ), the overlap of the emission of the LED and the absorption spectra of PS 1 and 2 are lower compared to that under blue-light irradiation although under green-light irradiation a higher spectral overlap is expected for PS 1 compared to that of PS 2. (Figure S10, the Supporting Information) For PS 1, the photocatalytic reaction rate and stability with green-light irradiation are approximatively the same as for blue-light irradiation. The hydrogen evolution under green-light irradiation of both systems (1–3 and 2–3) is different, a maximum TOF of  $30100 \text{ mmol}_{\text{H}_2} \text{ mol}_{\text{PS}}^{-1} \text{ min}^{-1}$  ( $\Phi_{\text{H}_2}=45.6\%$ ) is reached for 1 whereas this value is reduced to  $3500 \text{ mmol}_{\text{H}_2} \text{ mol}_{\text{PS}}^{-1} \text{ min}^{-1}$  ( $\Phi_{\text{H}_2}=9.5\%$ ) for 2 (Figure 6). The TON reaches a value of 7200 after 20 h of irradiation for 1 and 1100 after 19 h of irradiation for 2. Moreover, considering the quantity of TEOA used as SED ([TEOA]=1 M) and the fact that two electrons are given per oxidized TEOA molecule,<sup>[26]</sup> the photocatalytic system with [1]=0.1 mM converts, 78% and 72% of TEOA to H<sub>2</sub> under blue- and green-light irradiation, respectively.

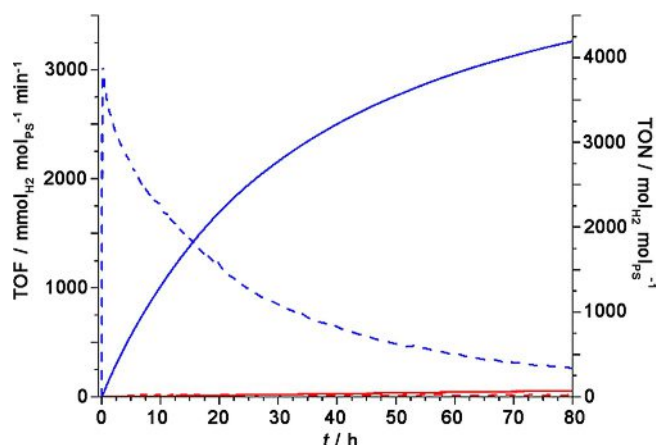


**Figure 6.** H<sub>2</sub> evolution of (1–3)+4 equiv. dmgh<sub>2</sub> (blue) and reference system (2–3)+4 equiv. dmgh<sub>2</sub> (red). 1 M TEOA as SED and 0.1 M HBF<sub>4</sub> as proton source were used for both systems in DMF. Solid line: TON, dashed line: TOF. Irradiation at 523 nm (green light).

In the case of PS 2, the rate of HER under green-light irradiation is fivefold lower under the same conditions (under blue-light irradiation) with only half the TON.

Under red-light irradiation ( $\lambda_{\text{em}}=630 \text{ nm}$ ), PS 1 exhibits a maximum TOF of  $3050 \text{ mmol}_{\text{H}_2} \text{ mol}_{\text{PS}}^{-1} \text{ min}^{-1}$  ( $\Phi_{\text{H}_2}=5.3\%$ ) to reach a TON of 4200 whereas the TON of hydrogen production for PS 2 reaches a maximum of 71 and the TOF is only 18 ( $\Phi_{\text{H}_2}=2.3\%$ ) after 80 h irradiation (Figure 7). Both systems are still active under irradiation after 80 h. To the best of our knowledge, the TOF and TON of PS 1 are the best values under red-light irradiation for a molecular photocatalytic HER.<sup>[8a, 14d]</sup> The tailing of the absorption spectra (Figure 4, inset) of PS 1 and 2 exhibits negligibly low molar absorptivity for both PS 1 and 2 in the red energy region ( $\lambda > 620 \text{ nm}$ ). Considering the lower absorptivity in the red energy region and the TOF, conversion of the absorbed photons to H<sub>2</sub> is still efficient compared to those under blue and green irradiation for PSs 1

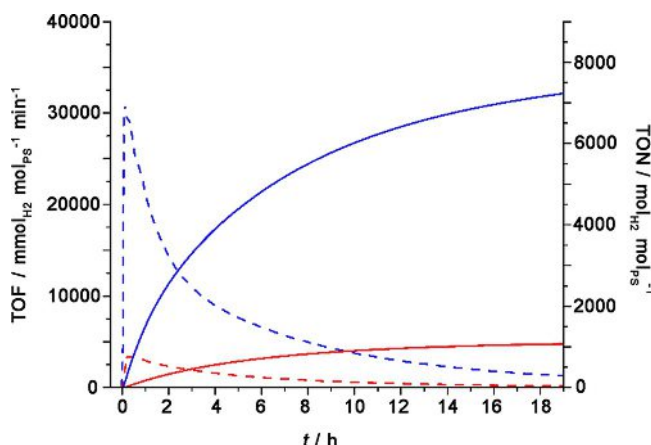


**Figure 7.** H<sub>2</sub> evolution of (1–3)+4 equiv. dmgh<sub>2</sub> (blue) and reference system (2–3)+4 equiv. dmgh<sub>2</sub> (red). 1 M TEOA as SED and 0.1 M HBF<sub>4</sub> as proton source were used for both systems in DMF. Solid line: TON, dashed line: TOF. Irradiation at 630 nm (red light).

and 2. Concerning a Ru–Pd dyad reported in the literature, wavelength-dependence studies for HER show that the catalytic efficiency of the TON is correlated with the direct population of the excited states upon excitation on MLCT.<sup>[11a]</sup> In our study, excitation in the red, green, and blue energy region of PS 1 promotes a <sup>3</sup>MLCT electronic transition from Ru<sup>II</sup> to L, which is also corroborated by the triplet spin density distribution of PS 1 in its excited state (Figure S8, the Supporting Information). For PS 1; green-light irradiation promotes population of the <sup>1</sup>MLCT and <sup>3</sup>MLCT states with L providing the lowest-energy LUMO. In this case, the quantum yield is relatively high:  $\Phi_{\text{H}_2}=46\%$ . Upon reduction of Co<sup>III</sup> to Co<sup>II</sup>, the chloride ion of catalyst 3 is free to bind in the amide pocket of L in PS 1. Once the chloride ion is in the pocket, 1 displays enhanced photophysical properties as described by Beer et al.<sup>[17]</sup> The transfer of the chloride ion to PS 1 would contribute to the enhanced photocatalytic H<sub>2</sub> evolution rate for PS 1 compared to PS 2.<sup>[15]</sup> At this point, however, PS 1 and photocatalyst 3 would not be in a supramolecular assembly.

In conclusion, we report a photocatalytic system with an amide-based Ru<sup>II</sup>-photosensitizer (PS) (1) and a cobaloxime-based catalyst [Co(dmgh)<sub>2</sub>(DMAP)Cl] (3, dmgh=dimethylglyoxime, DMAP=4-dimethylaminopyridine) that displays a high photocatalytic stability and rate of activity for the hydrogen evolution reaction. The photocatalytic system (1–3) was found to be highly efficient under both blue- and green-light irradiation conditions and also to be operative under red-light irradiation, albeit with a low quantum yield for the latter. The results were compared with [Ru(bpy)<sub>3</sub>]<sup>2+</sup> (2, bpy=2,2'-bipyridine) combined with catalyst 3. Under each irradiation conditions, 1 proves to be a more efficient PS than 2. Further investigations are underway to evaluate the impact of stronger H bonding for chloride anion and tuning of the photocatalyst for efficient H<sub>2</sub> production.

## Experimental Section

CCDC 1016847 contains the supplementary crystallographic data for this paper. These data can be obtained free of charge from The Cambridge Crystallographic Data Centre.

Synthetic, crystallographic, optoelectronic, DFT studies and experimental details of the HER are available in the Supporting Information.

## Acknowledgements

The authors thank the Natural Sciences and Engineering Research Council of Canada (NSERC) and Centre for Self-Assembled Chemical Structure (CSACS) for financial support.

## Conflict of interest

The authors declare no conflict of interest.

**Keywords:** hydrogen evolution • photocatalysis • solar fuel generation • supramolecular • transition metals

- [1] R. L. House, N. Y. M. Iha, R. L. Coppo, L. Alibabaei, B. D. Sherman, P. Kang, M. K. Brenneman, P. G. Hoertz, T. J. Meyer, *J. Photochem. Photobiol. C* **2015**, *25*, 32–45.
- [2] S. Berardi, S. Drouet, L. Francas, C. Gimbert-Surinach, M. Guttentag, C. Richmond, T. Stoll, A. Llobet, *Chem. Soc. Rev.* **2014**, *43*, 7501–7519.
- [3] V. Balzani, A. Credi, M. Venturi, *ChemSusChem* **2008**, *1*, 26–58.
- [4] a) S. Jasimuddin, T. Yamada, K. Fukuju, J. Otsuki, K. Sakai, *Chem. Commun.* **2010**, *46*, 8466–8468; b) A. Jacques, O. Schott, K. Robeyns, G. S. Hanan, B. Elias, *Eur. J. Inorg. Chem.* **2016**, 1779–1783; c) A. Fihri, V. Artero, A. Pereira, M. Fontecave, *Dalton Trans.* **2008**, 5567–5569; d) J. Liu, W. Jiang, *Dalton Trans.* **2012**, *41*, 9700–9707; e) B. F. DiSalle, S. Bernhard, J. Am. Chem. Soc. **2011**, *133*, 11819–11821; f) P. N. Curtin, L. L. Tinker, C. M. Burgess, E. D. Cline, S. Bernhard, *Inorg. Chem.* **2009**, *48*, 10498–10506; g) J. A. Porras, I. N. Mills, W. J. Transue, S. Bernhard, J. Am. Chem. Soc. **2016**, *138*, 9460–9472; h) D. R. Whang, K. Sakai, S. Y. Park, *Angew. Chem. Int. Ed.* **2013**, *52*, 11612–11615; *Angew. Chem.* **2013**, *125*, 11826–11829; i) S. A. Rommel, D. Sorsche, S. Schönweiz, J. Kübel, N. Rockstroh, B. Dietzek, C. Streb, S. Rau, *J. Organomet. Chem.* **2016**, *821*, 163–170; j) S. Schönweiz, S. A. Rommel, J. Kübel, M. Micheel, B. Dietzek, S. Rau, C. Streb, *Chem. Eur. J.* **2016**, *22*, 12002–12005; k) C. Lentz, O. Schott, T. Auvray, G. Hanan, B. Elias, *Inorg. Chem.* **2017**, *56*, 10875–10881; l) C. Lentz, O. Schott, T. Auvray, G. S. Hanan, B. Elias, **2017**, unpublished results.
- [5] a) A. Zarkadoulas, E. Koutsouri, C. Kefalidi, C. A. Mitsopoulou, *Coord. Chem. Rev.* **2015**, *304–305*, 55–72; b) H. Y. Wang, G. Si, W. N. Cao, W. G. Wang, Z. J. Li, F. Wang, C. H. Tung, L. Z. Wu, *Chem. Commun.* **2011**, *47*, 8406–8408.
- [6] a) P. Du, J. Schneider, G. Luo, W. W. Brennessel, R. Eisenberg, *Inorg. Chem.* **2009**, *48*, 4952–4962; b) S. Lin, K. Kitamoto, H. Ozawa, K. Sakai, *Dalton Trans.* **2016**, *45*, 10643–10654; c) X. Wang, S. Goeb, Z. Ji, N. A. Pogulachenko, F. N. Castellano, *Inorg. Chem.* **2011**, *50*, 705–707; d) K. Yamauchi, K. Sakai, *Dalton Trans.* **2015**, *44*, 8685–8696.
- [7] a) A. K. Pal, G. S. Hanan, *Chem. Soc. Rev.* **2014**, *43*, 6184–6197; b) C. V. Krishnan, B. S. Brunschwig, C. Creutz, N. Sutin, *J. Am. Chem. Soc.* **1985**, *107*, 2005–2015; c) C. V. Krishnan, N. Sutin, *J. Am. Chem. Soc.* **1981**, *103*, 2141–2142; d) J. Hawecker, J. M. Lehn, R. Ziessl, *Nouv. J. Chim.* **1983**, *7*, 271–277; e) L. Petermann, R. Staehle, M. Pfeifer, C. Reichardt, D. Sorsche, M. Wachtler, J. Popp, B. Dietzek, S. Rau, *Chem. Eur. J.* **2016**, *22*, 8240–8253; f) R. S. Khnayzer, B. S. Olaiya, K. A. El Roz, F. N. Castellano, *ChemPlusChem* **2016**, *81*, 1090–1097; g) M. W. Cooke, D. Chartrand, G. S. Hanan, *Coord. Chem. Rev.* **2008**, *252*, 903–921.
- [8] a) E. Rousset, D. Chartrand, I. Ciofini, V. Marvaud, G. S. Hanan, *Chem. Commun.* **2015**, *51*, 9261–9264; b) K. O. Johansson, J. A. Lotoski, C. C. Tong, G. S. Hanan, *Chem. Commun.* **2000**, 819–820; c) A. K. Pal, P. D. Ducharme, G. S. Hanan, *Chem. Commun.* **2014**, *50*, 3303–3305; d) A. K. Pal, G. S. Hanan, *Dalton Trans.* **2014**, *43*, 6567–6577; e) A. K. Pal, S. Nag, J. G. Ferreira, V. Brochery, G. La Ganga, A. Santoro, S. Serroni, S. Campagna, G. S. Hanan, *Inorg. Chem.* **2014**, *53*, 1679–1689; f) A. K. Pal, S. Serroni, N. Zaccheroni, S. Campagna, G. S. Hanan, *Chem. Sci.* **2014**, *5*, 4800–4811; g) A. K. Pal, N. Zaccheroni, S. Campagna, G. S. Hanan, *Chem. Commun.* **2014**, *50*, 6846–6849.
- [9] a) D. Z. Zee, T. Chantarojsiri, J. R. Long, C. J. Chang, *Acc. Chem. Res.* **2015**, *48*, 2027–2036; b) N. Queyriaux, R. T. Jane, J. Massin, V. Artero, M. Chavaroche-Kerlidou, *Coord. Chem. Rev.* **2015**, *304–305*, 3–19; c) S. Roy, M. Bacchi, G. Berggren, V. Artero, *ChemSusChem* **2015**, *8*, 3632–3638; d) A. Panagiotopoulos, K. Ladomenou, D. Sun, V. Artero, A. G. Coutsolelos, *Dalton Trans.* **2016**, *45*, 6732–6738.
- [10] a) H. Ozawa, M.-a. Haga, K. Sakai, *J. Am. Chem. Soc.* **2006**, *128*, 4926; b) H. Ozawa, K. Sakai, *Chem. Lett.* **2007**, *36*, 920–921; c) H. Ozawa, K. Sakai, *Chem. Commun.* **2011**, *47*, 2227–2242; d) H. Ozawa, Y. Yokoyama, M. A. Haga, K. Sakai, *Dalton Trans.* **2007**, 1197–1206; e) K. Sakai, H. Ozawa, *Coord. Chem. Rev.* **2007**, *251*, 2753–2766; f) T. Kowacs, L. O'Reilly, Q. Pan, A. Huijser, P. Lang, S. Rau, W. R. Browne, M. T. Pryce, J. G. Vos, *Inorg. Chem.* **2016**, *55*, 2685–2690; g) C. V. Suneesh, B. Balan, H. Ozawa, Y. Nakamura, T. Katayama, M. Muramatsu, Y. Nagasawa, H. Miyasaka, K. Sakai, *Phys. Chem. Chem. Phys.* **2014**, *16*, 1607–1616; h) M. G. Pfeffer, T. Kowacs, M. Wachtler, J. Guthmüller, B. Dietzek, J. G. Vos, S. Rau, *Angew. Chem. Int. Ed.* **2015**, *54*, 6627–6631; *Angew. Chem.* **2015**, *127*, 6727–6731; i) M. G. Pfeffer, B. Schafer, G. Smolentsev, J. Uhlig, E. Nazarenko, J. Guthmüller, C. Kuhnt, M. Wachtler, B. Dietzek, V. Sundstrom, S. Rau, *Angew. Chem. Int. Ed.* **2015**, *54*, 5044–5048; *Angew. Chem.* **2015**, *127*, 5132–5136.
- [11] a) Y. Halpin, M. T. Pryce, S. Rau, D. Dini, J. G. Vos, *Dalton Trans.* **2013**, *42*, 16243–16254; b) S. Rau, B. Schafer, D. Gleich, E. Anders, M. Rudolph, M. Friedrich, H. Gorls, W. Henry, J. G. Vos, *Angew. Chem. Int. Ed.* **2006**, *45*, 6215–6218; *Angew. Chem.* **2006**, *118*, 6361–6364; c) S. Tschieler, M. Presselt, C. Kuhnt, A. Yartsev, T. Pascher, V. Sundstrom, M. Karnahl, M. Schwalbe, B. Schafer, S. Rau, M. Schmitt, B. Dietzek, J. Popp, *Chem. Eur. J.* **2009**, *15*, 7678–7688; d) M. G. Pfeffer, C. Pehlken, R. Staehle, D. Sorrsche, C. Streb, S. Rau, *Dalton Trans.* **2014**, *43*, 13307–13315.
- [12] a) T. Stoll, M. Gennari, J. Fortage, C. E. Castillo, M. Rebarz, M. Sliwa, O. Poizat, F. Odobel, A. Deronzier, M. N. Collomb, *Angew. Chem. Int. Ed.* **2014**, *53*, 1654–1658; *Angew. Chem.* **2014**, *126*, 1680–1684; b) H. J. Sayre, T. A. White, K. J. Brewer, *Inorg. Chim. Acta* **2017**, *454*, 89–96; c) H. M. Rogers, S. M. Arachchige, K. J. Brewer, *Chem. Eur. J.* **2015**, *21*, 16948–16954; d) T. Stoll, C. E. Castillo, M. Kayanuma, M. Sandroni, C. Daniel, F. Odobel, J. Fortage, M.-N. Collomb, *Coord. Chem. Rev.* **2015**, *304–305*, 20–37; e) H. N. Kagawala, D. N. Chirdon, I. N. Mills, N. Budwal, S. Bernhard, *Inorg. Chem.* **2017**, *56*, 10162–10171.
- [13] a) V. Artero, M. Chavaroche-Kerlidou, M. Fontecave, *Angew. Chem. Int. Ed.* **2011**, *50*, 7238–7266; *Angew. Chem.* **2011**, *123*, 7376–7405; b) P. Du, J. Schneider, G. Luo, W. W. Brennessel, R. Eisenberg, *Inorg. Chem.* **2009**, *48*, 8646; c) N. Kaeffer, M. Chavaroche-Kerlidou, V. Artero, *Acc. Chem. Res.* **2015**, *48*, 1286–1295; d) M. Razavet, V. Artero, M. Fontecave, *Inorg. Chem.* **2005**, *44*, 4786–4795; e) P. Zhang, P.-A. Jacques, M. Chavaroche-Kerlidou, M. Wang, L. Sun, M. Fontecave, V. Artero, *Inorg. Chem.* **2012**, *51*, 2115–2120; f) S. Losse, J. G. Vos, S. Rau, *Coord. Chem. Rev.* **2010**, *254*, 2492–2504.
- [14] a) M. Schulz, M. Karnahl, M. Schwalbe, J. G. Vos, *Coord. Chem. Rev.* **2012**, *256*, 1682–1705; b) K. L. Mulfort, C. R. Chim. **2016**, *20*, 221–229; c) K. L. Mulfort, L. M. Utschig, *Acc. Chem. Res.* **2016**, *49*, 835–843; d) E. Rousset, I. Ciofini, V. Marvaud, G. S. Hanan, *Inorg. Chem.* **2017**, *56*, 9515–9524.
- [15] E. Deponti, M. Natali, *Dalton Trans.* **2016**, *45*, 9136–9147.
- [16] O. S. Wenger, *Coord. Chem. Rev.* **2009**, *293*, 1439–1457.
- [17] a) P. D. Beer, S. W. Dent, T. J. Wear, *J. Chem. Soc. Dalton Trans.* **1996**, 2341–2346; b) P. D. Beer, F. Szemes, V. Balzani, C. M. Sala, M. G. B. Drew, S. W. Dent, M. Maestri, *J. Am. Chem. Soc.* **1997**, *119*, 11864–11875.
- [18] C. Lopez, J.-C. Moutet, E. Saint-Aman, *J. Chem. Soc., Faraday Trans.* **1996**, *92*, 1527–1532.
- [19] A. Brown, P. D. Beer, *Chem. Commun.* **2016**, *52*, 8645–8658.
- [20] F. H. Allen, *Acta Crystallogr. Sect. B* **2002**, *58*, 380–388.
- [21] J. W. Slater, D. M. D'Alessandro, F. R. Keene, P. J. Steel, *Dalton Trans.* **2006**, 1954–1962.

- [22] A. Juris, V. Balzani, F. Barigelletti, S. Campagna, P. Belser, A. von Zelewsky, *Coord. Chem. Rev.* **1988**, *84*, 85–277.
- [23] K. Suzuki, A. Kobayashi, S. Kaneko, K. Takehira, T. Yoshihara, H. Ishida, Y. Shiina, S. Oishi, S. Tobita, *Phys. Chem. Chem. Phys.* **2009**, *11*, 9850–9860.
- [24] a) D. Basu, S. Mazumder, J. Niklas, H. Baydoun, D. Wanniarachchi, X. Shi, R. J. Staples, O. Poluektov, H. B. Schlegel, C. N. Verani, *Chem. Sci.* **2016**, *7*, 3264–3278; b) M. A. W. Lawrence, M. J. Celestine, E. T. Artis, L. S. Joseph, D. L. Esquivel, A. J. Ledbetter, D. M. Cropek, W. L. Jarrett, C. A. Bayse, M. I. Brewer, A. A. Holder, *Dalton Trans.* **2016**, *45*, 10326–10342.
- [25] D. W. Wakerley, E. Reisner, *Phys. Chem. Chem. Phys.* **2014**, *16*, 5739–5746.
- [26] B. Probst, A. Rodenberg, M. Guttentag, P. Hamm, R. Alberto, *Inorg. Chem.* **2010**, *49*, 6453–6460.

---

Manuscript received: August 15, 2017

Revised manuscript received: September 21, 2017

Accepted manuscript online: September 25, 2017

Version of record online: October 16, 2017

---